

InGaAs quantum dot molecules around self-assembled GaAs nanomound templates

J. H. Lee, Zh. M. Wang,^{a)} N. W. Strom, Yu. I. Mazur, and G. J. Salamo
Physics Department, University of Arkansas, Fayetteville, Arkansas 72701

(Received 24 July 2006; accepted 29 August 2006; published online 13 November 2006)

Several distinctive self-assembled InGaAs quantum dot molecules (QDMs) are studied. The QDMs self-assemble around nanoscale-sized GaAs moundlike templates fabricated by droplet homoepitaxy. Depending on the specific InAs monolayer coverage, the number of QDs per GaAs mound ranges from two to six (bi-QDMs to hexa-QDMs). The Ga contribution from the mounds is analyzed in determining the morphologies of the QDMs, with respect to the InAs coverages ranging between 0.8 and 2.4 ML. Optical characterization shows that the resulting nanostructures are high-quality nanocrystals. © 2006 American Institute of Physics. [DOI: 10.1063/1.2388049]

To fabricate nanostructures under an insufficient lattice mismatch, a growth technique, called “droplet epitaxy,” was introduced for homoepitaxial and heteroepitaxial material systems, such as GaAs/GaAs and GaAs/Al(Ga)As.^{1–6} In droplet epitaxy, under the absence of an As₄ flux, a molecular beam of Ga applied to a surface forms liquid Ga droplets based on Volmer-Weber growth mode.⁷ These droplets are then subsequently exposed to an As₄ flux and crystallized to form GaAs. However, this process can be substantially more complicated and interesting. For example, a GaAs/Al(Ga)As droplet epitaxy results in various shapes depending on the growth conditions during the As₄ annealing process of the liquid Ga droplets. Some of these droplets form elongated islands along [01-1], both with and without nanoscale holes, while other droplets form single and double ringlike nanostructures.^{4–6}

These various shape droplets can subsequently serve as templates for further growth, without the need for further *ex situ* surface preparation. This approach overcomes several limitations of typical quantum dot (QD) growth on planar GaAs surfaces.^{1–6} This can be significant since semiconductor QDs have received considerable attention due to their unique electronic and optoelectronic properties.^{8–12} In fact, several important devices have already been demonstrated using QDs, such as lasers, transistors, sensors, and photodetectors.^{13–15} Furthermore, the use of the spin of an electron as a basic unit for quantum computations is intensely being explored using both electrical and optical techniques to localize and manipulate a single spin in QDs.^{16–21}

For this application, traditional self-assembly of QDs based on the Stranski-Krastanov (SK) growth mode can be a good candidate for quantum computations.^{18–21} Characteristically, however, SK-based growth generally has random lateral spacing, which hinders the QD functionality for such applications as a *q* bit.

In this letter, we adopt a hybrid growth approach utilizing both droplet homoepitaxy and SK growth to overcome some of the limitations of the SK-based QD growth mode alone on a planar GaAs surface. Using molecular beam epitaxy (MBE) self-assembled InGaAs quantum dot molecules (QDMs) are realized around GaAs mounds formed by droplet epitaxy on GaAs (100). The number of QDs per GaAs

mound can be effectively controlled by varying the InAs monolayer coverage. For example, we demonstrate QDMs composed of two to six QDs per mound. Physically, we find that intermixing of Ga from the GaAs mounds contributes to the morphology of the InGaAs QDMs. This behavior is systematically analyzed from the initial mixing stage to the near elimination of the GaAs mounds. The corresponding photoluminescence (PL) measurements indicate that the InGaAs QDMs are high-quality crystalline nanostructures.

All samples were grown on epitaxy-ready semi-insulated GaAs (100) substrates by solid-source MBE. After 330 nm of GaAs buffer, 3 ML of Ga (based on an equivalent amount of GaAs with As₄ flux) was applied to the GaAs surface at the surface temperature of 500 °C without As₄ flux to form liquid Ga droplets on the GaAs surface. Subsequently, 80 s of annealing followed, and the substrate temperature was lowered to 150 °C. The Ga droplets were then exposed to a beam equivalent pressure (BEP) of 1.3×10^{-5} Torr of As₄ for 100 s in order to fully crystallize the Ga droplets and to

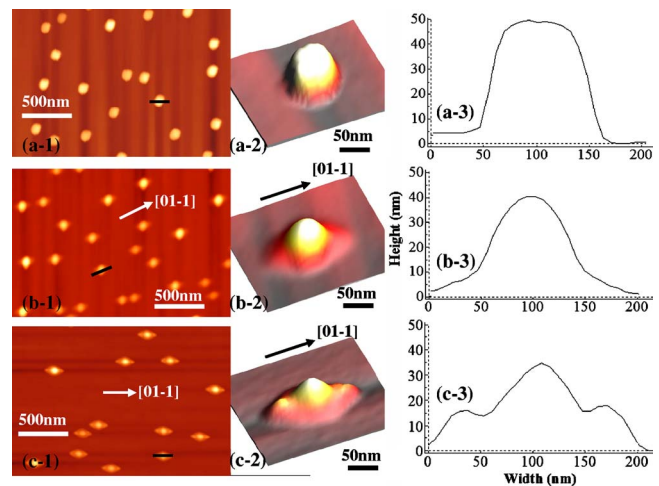


FIG. 1. (Color online) Surface morphology [two dimensional and three dimensional (3d)] by AFM and corresponding line profiles indicated as black lines in Figs. (a-1), (b-1), and (c-1). The InAs monolayer coverage is varied: (a) 0.0 ML, (b) 0.8 ML, and (c) 1.4 ML deposition at 500 °C after 3 ML of Ga deposition at 500 °C (equivalent amount of GaAs when As₄ was supplied) and crystallization at 150 °C. Figures (a-1), (b-1), and (c-1) are $2(x) \times 1.5(y) \mu\text{m}^2$, and Figs. (a-2), (b-2), and (c-2) are $300(x) \times 250(y) \text{nm}^2$. Black lines in the $2 \times 1.5 \mu\text{m}^2$ figures correspond to the line profiles shown in Figs. (a-3), (b-3), and (c-3).

^{a)}Electronic mail: zmwang@uark.edu

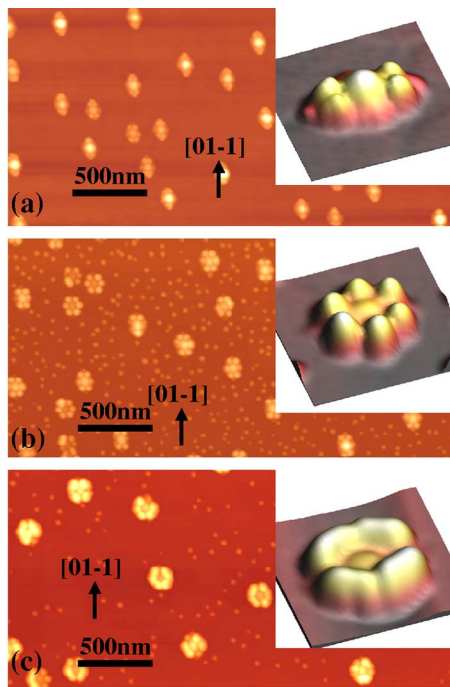


FIG. 2. (Color online) AFM images of (a) 1.6 ML, (b) 2.0 ML, and (c) 2.4 ML of InAs deposition at 500 °C. InAs QDs were deposited after 3 ML of Ga deposition at 500 °C (equivalent amount of GaAs when As_4 was supplied) and crystallization at 150 °C. Inserted enlarged 3D AFM images are the major structures (most dominant structures) for the given sample. Figures are $3(x) \times 1.5(y) \mu\text{m}^2$, and insertions are $300 \times 300 \text{ nm}^2$.

form the GaAs nanoscale mound templates. The substrate temperature was raised to 500 °C and InAs deposition followed. Under a BEP of 3.4 μTorr of As_4 , the monolayer coverage of InAs was deposited ranging from 0.8 to 2.4 ML. The substrate temperature was then quenched under the same BEP of As_4 flux as was used during the InAs growth. For PL measurements, a 200 ML of GaAs capping layer was grown, and the measurements were carried out at 10 K using a 532 nm (2.33 eV) laser excitation. Meanwhile, an atomic force microscope (AFM) was also used on uncapped samples to reveal the surface morphology.

In all our experiments, the GaAs mounds formed with 3.0 ML Ga deposition, shown in Figs. 1(a-1)–1(a-3), were used as the templates for the subsequent InAs depositions. In other reported cases,^{3–6} noncircular shapes of crystallized GaAs islands were explained by anisotropic surface diffusion of Ga atoms along the [01-1] and [011] directions during the crystallization. To minimize the effects of anisotropic surface diffusion of Ga atoms during crystallization, Ga droplets were crystallized at the substrate temperature of 150 °C. This is much lower than the substrate temperature of 450 to 550 °C used in previous reports.^{3–6} The density of the GaAs island templates was $\sim 1.6 \times 10^7/\text{cm}^2$, and the average dimensions of the templates were $\sim 120 \text{ nm}$ in diameter and $\sim 50 \text{ nm}$ in height. The formation of the GaAs nanomounds was then followed with various monolayer depositions the InAs coverage. Figures 1(b-1)–1(b-3) show the resulting surface morphology and line profiling after 0.8 ML of InAs deposition. The height of the GaAs mound decreased by $\sim 10 \text{ nm}$ from the original mounds to $\sim 40 \text{ nm}$, and the diameter decreased to $\sim 90 \text{ nm}$. From the enlarged Fig. 1(b-2) and the line profile in Fig. 1(b-3), it appears that the InAs growth started mixing with the Ga atoms from the GaAs

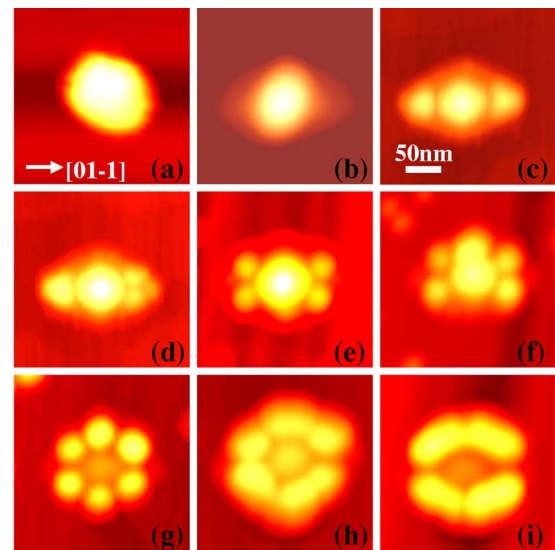


FIG. 3. (Color online) Evolution of the QDMs from the GaAs mounds to the structures: (a) GaAs mound, (b) InAs shoulder, (c) bi-, (d) tri-, (e) quad-, (f) penta-, (g) hexa-molecules, and (h) a large hexa-QDM, and (i) a molecule with elongated nanostructures. All figures are $250 \times 250 \text{ nm}^2$, and the crystallographic direction in (a) and the scale bar in (c) are applied to the other images. InAs monolayer coverages associated with the acquisition of sample figures were as follows: (a) 0 ML, (b) 0.8 ML, (c) 1.4 ML, [(d) and (e)] 1.6 ML, [(f) and (g)] 2.0 ML, and [(h) and (i)] 2.4 ML.

mounds, resulting in InGaAs shoulders on initial templates along the [01-1] and [0-11] directions. As shown in Figs. 1(c-1)–1(c-3), by increasing the InAs coverage to 1.4 ML, two QDs (QDM) clearly appeared for each GaAs mound along the [01-1] and [0-11] directions. This is likely due to the anisotropic surface diffusion of the adatoms and to the asymmetric (2×4) reconstruction of the GaAs (100) surface. The percentage of GaAs mounds that supported two QDs was $\sim 95\%$, while the other $\sim 5\%$ formed three QDs. The average QD height and diameter of the two-dot QDMs were ~ 18 and $\sim 60 \text{ nm}$, respectively. The observed decrease in height and volume of the GaAs mounds seen in Fig. 1(c-3) indicates that the Ga atoms mixed with the InAs QDs.

Figures 2(a)–2(c) show the results of further increase in the InAs monolayer coverage, with 1.6, 2.0, and 2.4 ML deposition grown at a substrate temperature of 500 °C. In Fig. 2(a), 1.6 ML InAs deposition resulted in an increase in the number of major QDs per mound to four (quad-QDMs). While $\sim 75\%$ were quad-QDMs, $\sim 25\%$ of these nanostructures formed tri-QDMs. Thus with this amount of monolayer coverage, the QDMs were less uniform than in the 1.4 ML deposition. The average QD heights and diameters of the quad-QDMs were ~ 15 and $\sim 55 \text{ nm}$, respectively. Meanwhile, with 2.0 ML of coverage, shown in Fig. 2(b), hexa-QDMs (six QDs) were formed, with very good uniformity in the number of QDs per mound ($\sim 90\%$). In this sample, the average QD heights and diameters were ~ 20 and $\sim 60 \text{ nm}$, respectively. 2.4 ML InAs deposition, however, shown in Fig. 2(c), caused a merging of the QDs in each GaAs mound, resulting in elongated nanostructures. The average height of these nanostructures was $\sim 33 \text{ nm}$. In comparing the GaAs mound heights in these samples, the 1.6 ML sample was $\sim 30 \text{ nm}$, the 2.0 ML sample was $\sim 22 \text{ nm}$, and the 2.4 ML sample was $\sim 18 \text{ nm}$. Thus, with an increasing deposition of InAs, the GaAs mound size kept decreasing, which further

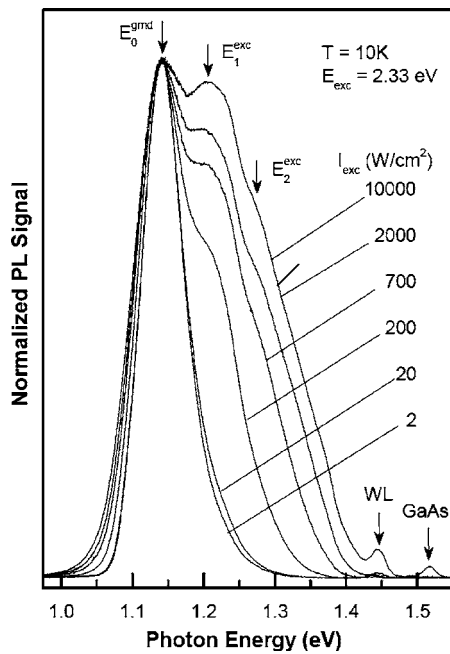


FIG. 4. PL spectra of InGaAs QDMs formed around nanoscale GaAs mound templates with 1.6 ML of InAs deposition at 500 °C. The surface morphology is shown in Fig. 2(a). Six spectra peaks cover the range of laser power densities from P_0 to $(5 \times 10^3) \times P_0$, where P_0 is 2 W/cm². The vertical arrows indicate the evolution of the PL peak from the ground state (E_0) to the first (E_1) and the second excited states (E_2).

supports the claim of Ga atom intermixing with the InAs QDs.

Figures 3(a)–3(i) show the evolution of the QDMs from GaAs mounds into bi-QDMs, to hexa-QDMs, and finally into the elongated nanostructures. The original GaAs mound, as shown in Fig. 3(a), is more or less rounded in shape. Due to surface anisotropy of the GaAs (100) surface, the deposited InAs tended to mix with GaAs along the [01-1] and [0-11] directions. This process leads to the emergence of the shoulders in Fig. 3(b) and the formation of a bi-QDM along [01-1] and [0-11], as seen in Fig. 3(c). With additional InAs deposition, the InGaAs QDs in the bi-QDMs increased in size and in surface strain. Finally, one QD in the bi-QDM split into two, forming tri-QDM, as seen in Fig. 3(d) and when both QDs in the bi-QDM split, a quad-QDM was observed, as in Fig. 3(e). Some additional InAs deposition builds up as shoulders along [011] and [0-1-1] in the quad-QDMs shown in Fig. 3(e). When one shoulder developed into a QD, the quad-QDM became a penta-QDM, as in Fig. 3(f) and if both shoulders developed into QDs, the hexa-QDM formed, as in Fig. 3(g). Continued InAs deposition encouraged the QDs in the hexa-QDMs to further increase in size, as shown in Fig. 3(h), until finally they formed the elongated nanostructures, as in Fig. 3(i).

Figure 4 shows the QDM PL data from the sample of 1.6 ML InAs deposition capped with 300 nm GaAs. This monolayer deposition resulted in InGaAs quad-molecules as shown in Fig. 2(a). With the low excitation intensity of 2 W/cm², the PL emission represents a single line from the ground state transition centered at 1.15 eV. The very high signal to noise ratio at such low excitation intensity shows that QDMs are rather good quality nanocrystals. The PL line spectral position also supports the contribution of Ga atoms

from GaAs mounds to InAs QDs as described previously. In general, for pure InAs QD with such dimensions (~ 15 nm in height and ~ 55 nm in diameter), a redshift is expected.²² The full width at half maximum of the PL spectra was about 60 meV. With increasing excitation intensity up to 3.5 orders, first (E_1) and second (E_2) excited states showed up. We believe that this QDM sample as well as others discussed above would be perfect candidates for single QDM spectroscopy investigation.

In summary, to create InGaAs QDMs on GaAs nanoscale-sized mound templates, a hybrid growth approach was adopted by combining droplet homoepitaxy (GaAs nanomounds on planar GaAs) and SK-based QD growth mode (InAs on the GaAs nanomounds). Using this approach, we demonstrated a progression from an initially rounded GaAs mound to a bi-QDM (with 1.8 ML) and then to a hexa-QDM (with 2.5 ML). Further increase in InAs monolayer deposition led to an elongated QD molecule. The PL results showed that the nanostructures grown were high-quality nanocrystals. Further studies are now underway to capture the PL spectra of single molecules.

The authors acknowledge the financial support of the NSF through Grant No. DMR-0520550 and the ONR through Grant No. N00014-00-1-0506.

- ¹Z. Gong, Z. C. Niu, S. S. Huang, Z. D. Fang, B. Q. Sun, and J. B. Xia, *Appl. Phys. Lett.* **87**, 093116 (2005).
- ²Zh. M. Wang, K. Holmes, J. L. Shultz, and G. J. Salamo, *Phys. Status Solidi A* **202**, R85 (2005).
- ³J. Planelles and J. I. Climente, *Eur. Phys. J. B* **48**, 65 (2005).
- ⁴B. L. Liang, Zh. M. Wang, J. H. Lee, K. Sablon, Yu. I. Mazur, and G. J. Salamo, *Appl. Phys. Lett.* **89**, 043133 (2006).
- ⁵J. H. Lee, Zh. M. Wang, Z. Y. AbuWaar, N. W. Strom, and G. J. Salamo, *Nanotechnology* **17**, 3973 (2006).
- ⁶T. Mano, T. Kuroda, S. Sanguinetti, T. Ochiai, T. Tateno, J. Kim, T. Noda, M. Kawabe, K. Sakoda, G. Kido, and N. Koguchi, *Nano Lett.* **5**, 425 (2005).
- ⁷M. Volmer and A. Weber, *Z. Phys. Chem.* **119**, 277 (1926).
- ⁸Jae-Young Lee, Minhyun Jeon, Jewon Lee, Guansik Cho, Jong Su Kim, Se-Kyung Kang, S. I. Ban, J. I. Lee, and Hyung Koun Cho, *J. Cryst. Growth* **252**, 493 (2003).
- ⁹Takashi Hanada and Hirofumi Totsuka, *J. Vac. Sci. Technol. B* **24**, 1886 (2006).
- ¹⁰H. Shin, J. B. Kim, Y. H. Yoo, W. Lee, E. Yoon, and Y. M. Yu, *J. Appl. Phys.* **99**, 023521 (2006).
- ¹¹E. E. Vdovin, A. Levin, A. Patanè, L. Eaves, P. C. Main, Yu. N. Khanin, Yu. V. Dubrovskii, M. Henini, and G. Hill, *Science* **290**, 122 (2000).
- ¹²M. Richter, B. Damilano, J.-Y. Duboz, and J. Massies, *Appl. Phys. Lett.* **88**, 231902 (2006).
- ¹³W. J. Choi, J. D. Song, J. I. Lee, K. C. Kim, and T. G. Kim, *Physica B* **376/377**, 886 (2006).
- ¹⁴X. Q. Li, Y. W. Wu, D. Steel, D. Gammon, T. H. Stievater, D. S. Katzer, D. Park, C. Piermarocchi, and L. J. Sham, *Science* **301**, 809 (2003).
- ¹⁵D. J. Mowbray and M. S. Skolnick, *J. Phys. D* **38**, 2059 (2005).
- ¹⁶G. D. Sanders, K. W. Kim, and W. C. Holton, *Phys. Rev. A* **60**, 4146 (1999).
- ¹⁷A. Imamoglu, *Physica E (Amsterdam)* **16** 47 (2003).
- ¹⁸K. R. Brown, D. A. Lidar, and K. B. Whaley, *Phys. Rev. A* **65**, 012307 (2001).
- ¹⁹Xuedong Hu and S. Das Sarma, *Phys. Rev. A* **64**, 042312 (2001).
- ²⁰S. S. Li, G. L. Long, F. S. Bai, S. L. Feng, and H. Z. Zheng, *Proc. Natl. Acad. Sci. U.S.A.* **98**, 11847 (2001).
- ²¹Rudeesun Songmuang, Suwit Kiravittaya, and Oliver G. Schmidt, *Appl. Phys. Lett.* **82**, 2892 (2003).
- ²²Yalin Ji, Wei Lu, Guibin Chen, Xiaoshuang Chen, and Qing Wang, *J. Appl. Phys.* **93**, 1208 (2003).